Structural Engineering and Mechanics, *Vol. 75, No. 6 (2020) 785-797*
DOI: https://doi.org/10.12989/sem.2020.75.6.785

Investigation of the refined safety factor for berthing energy calculation

Sang Woo Kim[1,2a], Seung Jae Lee[1b], Young Tae Kim[3a] and Do Kyun Kim*[2,4,5]

[1]Offshore Plant Engineering Laboratory, Division of Naval Architecture and Ocean Systems Engineering, Korea Maritime and Ocean University, 49112 Busan, Republic of Korea
[2]Ocean & Ship Technology, Department of Civil and Environmental Engineering, Universiti Teknologi PETRONAS, 32610 Seri Iskandar, Perak, Malaysia
[3]Daewoo Institute of Construction Technology, 16297 Suwon, Republic of Korea
[4]Group of Marine Offshore and Subsea Technology, School of Engineering, Newcastle University, NE1 7RU Newcastle upon Tyne, United Kingdom
[5]Graduate Institute of Ferrous Technology, Pohang University of Science and Technology, 37673 Pohang, Republic of Korea

(Received September 23, 2018, Revised April 3, 2020, Accepted May 18, 2020)

Abstract. As the growth of world trade has surged rapidly over the past years, the number is expected to continue growing over the coming years. Although the transportation costs can be reduced by using larger vessels, however, new berthing structures have to be constructed in order to cater for the larger vessels. This leads to a need for researching on designing a better berthing structure. For optimization of berthing structure design, we need to provide a better estimation of berthing energy than the previous methods in the existing guidelines. In this study, several berthing parameters were collected from previous works and researches. Moreover, the scenarios were selected efficiently by using a sampling technique. First, the berthing energy was calculated by executing 150 numerical simulations. Then, the numerical simulation results were compared with the results calculated by existing methods quantitatively to investigate the sensitivity of the berthing parameters and the accuracy of existing methods. The numerical method results have shown some deviation with respect to the existing method results in which the degree of deviation varies with the methods and the tendency of differences is dependent on certain berthing parameters. Then, one of the existing methods which has shown a small deviation was selected as a representative method and applied with several safety factors to obtain a suitable safety factor for the design.

Keywords: berthing energy, kinematic energy method, berthing velocity, berthing angle, safety factor

1. Introduction

Over the past decades, the growth of world trade has been increasing continuously. The size of the vessels has also become larger in order to reduce transportation costs. Depending on the type of cargos, the vessels berth at different types of berthing structures and the number of new berthing structures is gradually increasing (Mostofi and Bargi 2012). During berthing, the kinetic energy of the ship is absorbed by the fender system, which the amount of kinetic energy of the ship absorbed by the fender is defined as the berthing energy (Metzger *et al.* 2014). To optimize the design parameters and enhance the quality of the berthing structures, an accurate estimation of the berthing energy of a ship is needed (Roubos *et al.* 2018). Generally, there are several kinds of research related to berthing energy estimation.

The first method is an experimental study mainly used to identify the interaction effect between ships and structures. However, it is difficult to describe a viscous effect of reduced models on an experiment. Hence, this method is deemed inaccurate. The second method is an empirical method to determine the value of the design parameter using the measurements. Using this method, Girgrah (1977) proposed a formula for calculating the berthing energy with a ship's volumetric displacement.

In the Computational Fluid Dynamics (CFD) method, an added mass term that is related to the hydrodynamic force of kinetic energy method equation and fluid effect occurs during berthing was analyzed by using CFD software. In a previous study (Chen and Chen 1996), the CFD method for analyzing berthing was validated for the first time. This method was applied to analyze transient fluid force during berthing (Toda *et al*. 2002). In addition, Kong *et al.* (2004) emphasized the importance of the added mass term in the shallow water in this study. A research done by Wang *et al.* (2016, 2017) has taken into account the quay wall and free surface effects in a CFD study. However, this method is demanding lots of memories and long computing time for analysis.

The statistical method is utilized to reflect the investigated field berthing data to the design of new berthing structures and to derive the realistic probabilistic distribution of berthing variables. In a related study, according to statistical data measured by a large seagoing vessel at Bremerhaven (Hein 2014) and Rotterdam harbor (Roubos *et al.* 2017), it was proven that the berthing velocity was affected by a variety of variables instead of being just deadweight tonnage (DWT) dependent by the

*Corresponding author, Senior Lecturer, Adjunct Professor
E-mail: do.kim@ncl.ac.uk; dokim@postech.ac.kr
[a] Researcher
[b] Professor

ISSN: 1225-4568 (Print), 1598-6217 (Online)

Roubos *et al.* (2017). Yamase *et al.* (2014) studied that the berthing velocities are not influenced by types of berthing structure and fender. In Japan, the fender design guidelines had been improved by statistical research related to the safety factor applied to exist fender structures (Ueda *et al.* 2002). A statistical study was also performed on the frequency and size of Liquefied Natural Gas (LNG) tankers berth the jetty system (Saurin 1963, Toppler and Weersma 1973). However, since large deviations were observed in actual data, it was difficult to be applied directly to the new design for the berthing structure. To overcome these limitations and improve the guidelines, the Permanent International Association of Navigation Congresses (PIANC) has established a working group MarCom 145 and collected large quantities of statistical data pertaining to berthing parameters since 2002 from the major ports over the world (Burkhart and Matakis 2013).

The last method is an analytical method. In general, this method is still in development and rarely being compared with real berthing data. However, this method can be used for designing of berthing structure. This method requires a high-level numerical simulation based on practical evidence in order to be accurate. An impulse response function was used for berthing simulation to illustrate the interaction between the ship and the quay on still water without any environmental condition (Fontijn 1988). Headland (1992a, b) compared the results obtained from the mathematical analysis with those collected from the field measurement. Some of the analysis results were similar to the measurement but the data trend was inconsistent and hard to be proven perfectly. Also, the ferries berthing simulation was carried out using the actual fluid structural software (Neser and Unsalan 2006). Coupled simulations of the tanker and elastic pile-fender were performed using the interactive treatment method (ITM) to consider an interaction between a fender and structure (Magda 2019).

The common approaches for designing berthing structures are analytical and statistical methods. The existing berthing structure and fender design guidelines (ROM 1990, PIANC 2002, Grabe 2012, BS6349-4 2014) are based on these methods and the kinetic energy method is used to estimate the berthing energy. However, various coefficients in the equation do not reflect the recent measurements and many assumptions are used in estimating the berthing energy.

In this study, the berthing energy obtained by the numerical simulations was compared with those of the conventional methods to evaluate the difference between two methods quantitatively. In order to select reliable simulation scenarios, the statistical data related to the berthing parameters were investigated. In the comparison, the range of berthing energy, quantitative difference between two methods, and the sensitivity of berthing energy according to berthing variable were investigated. In addition, a refined safety factor is proposed based on the above results.

In section 2, the generalized procedure for the berthing energy comparison is illustrated. The details of berthing parameters and values, the ship and berthing structure modeling, and the simulation scenarios are described in section 3. In addition, the comparison results and the refined safety factor is represented in section 3. The main conclusions are discussed in section 4.

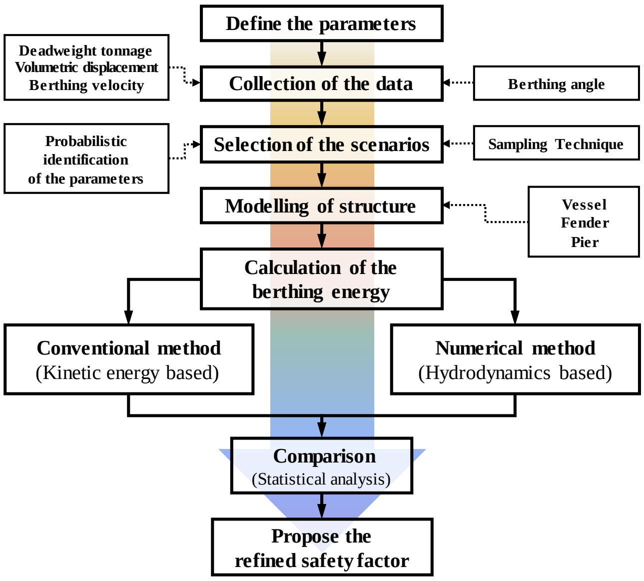

Fig. 1 Procedure to compare the berthing energy calculation methods

2. Procedure for the berthing energy comparison

The main works in this paper are refining the safety factor for berthing energy calculation by comparing the berthing energy calculation methods. The empirical formulation-based method which had been applied in fender design is designated the conventional method, or kinetic energy method, herein. On the other hand, the berthing energy calculation using the ANSYS-AQWA, which is for the hydrodynamic force calculation acting on the submerged body based on the potential theory is chosen as the numerical method (ANSYS 2013).

Based on the achieved comparison results between conventional and numerical methods, the proposed refined safety factor may help to prevent overdesign of the fender structures. The procedure to propose the refined safety factor through a comparison between the conventional and numerical methods is shown in Fig. 1.

The parameters related to berthing energy calculation is to be defined in the first step. Once the required parameters are defined, data such as DWT, volumetric displacement of the ship, berthing velocity, berthing angle can be collected. In order to achieve reliable comparison, the reasonable scenarios should be constructed through probabilistic identification of the investigated statistical data. In addition, a sampling technique is required to efficiently reduce the number of scenarios, this helps to manage the berthing energy calculation through cost-effective numerical simulations.

The structural modeling and calculation of the berthing energy are performed based on the selected reliable scenarios. Once the comparison between the two methods has been done, the refined safety factor can be proposed.

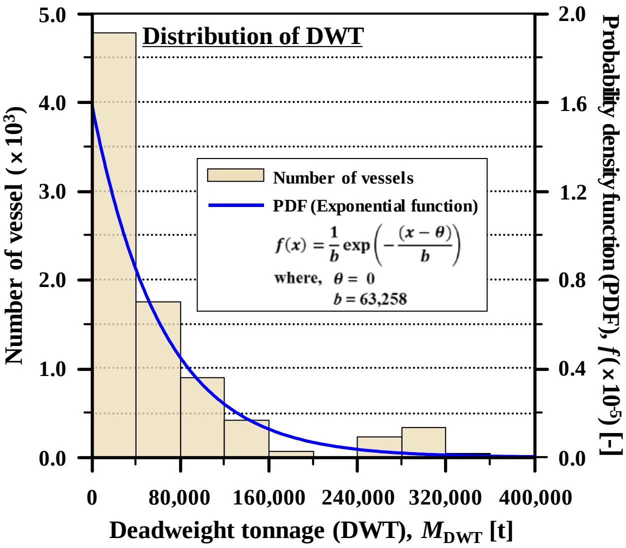

Fig. 2 Distribution of the number of tankers with respect to the deadweight tonnage

The proposed procedure is verified by the applied example in the next section.

3. Applied example

3.1 Define the parameters & Collection of the data

The LNG-carrier is selected as the vessel type while four types of berthing parameters are selected. The values of each parameter are investigated with reference to existing research and real statistical data.

3.1.1 DWT and volumetric displacement

DWT is the weight of cargo that can be loaded onto the ship and it is one of the parameters for calculating the berthing energy. According to the guidelines, the berthing velocity or volumetric displacement can be estimated from the DWT. The number of vessels according to the DWTs in the world (Clarkson 2014), and the tanker's histogram and the probability density function with respect to the DWT are shown in Fig. 2.

The volumetric displacement refers to the weight or volume of water displaced by the ship, which is a different concept from DWT. Based on the statistical data with reference to the guidelines (PIANC 2002), the volumetric displacement can be estimated according to the type of ships and its confidence limit level by using DWT as a variable. Fig. 3 shows a DWT and volumetric displacement relationship of the LNG carrier provided from the guidelines, which can be represented throughout the Eqs. (1) to (3). 50% and 75% are utilized in a normal design while 95% is used for extreme condition design.

For confidence limit 50%

$$V_D = 5.12(M_{DWT})^{0.88} \tag{1}$$

For confidence limit 75%

$$V_D = 5.55(M_{DWT})^{0.88} \tag{2}$$

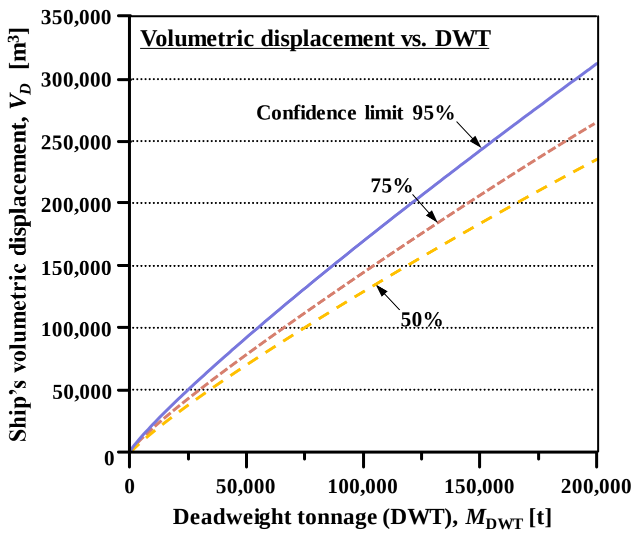

Fig. 3 DWT and volumetric displacement relationship for LNG ships

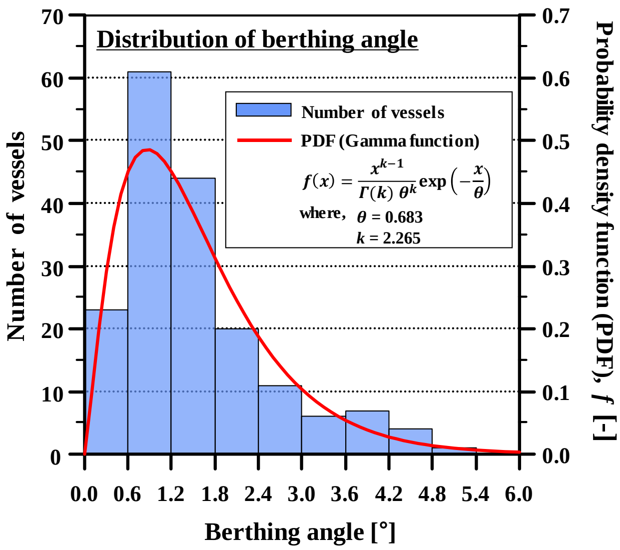

Fig. 4 Distribution of the number of vessels with respect to the berthing angles

For confidence limit 95%

$$V_D = 6.61(M_{DWT})^{0.88} \tag{3}$$

where V_D is the ship's volumetric displacement (m^3) and M_{DWT} is the ship's deadweight tonnage (t).

3.1.2 Berthing angle

According to the guidelines, a berthing case with an approach angle less than 6° is classified as small berthing, and, this is the cases that are considered in this study. The data of berthing angles and the number of ships are taken from a previous study (Roubos *et al.* 2017) which is based on the measurement at the port at Notre Dame. However, the actual measurement data provided in the reference were only in a considerably smaller berthing angle range below 1.5^0. In order to make the various small berthing scenarios, it was scaled up to 6^0. The distribution of the berthing angle respect to the ship number is shown in Fig. 4.

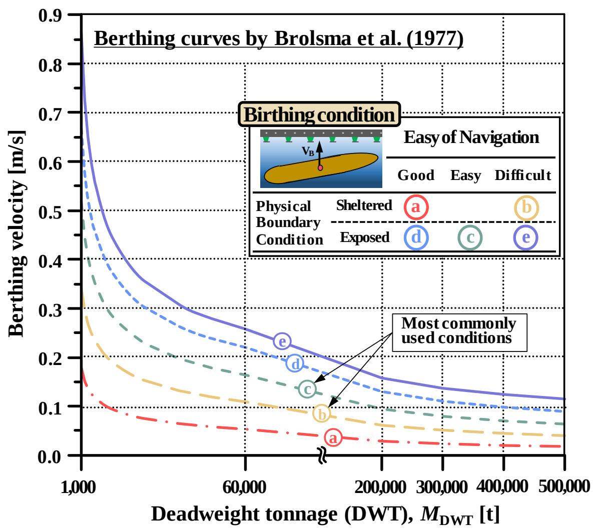

Fig. 5 Brolsma's berthing curves

Table 1 LNG-carrier dimension and mass properties

Parameters	Values
Length between perpendiculars, L_{BP} [m]	270
Breadth, B [m]	43.4
Draught, D [m]	11.916
Volumetric displacement, V_D [m^3]	102,591
Radius of gyration, k_{xx} [m]	15.703
Radius of gyration, k_{yy} [m]	67.5
Radius of gyration, k_{zz} [m]	69.302
Longitudinal center of gravity (to FP) [m]	-0.122
Vertical center of gravity [m]	4.43

3.1.3 Berthing velocity

The Brolsma curve (Brolsma *et al.* 1977) is used to determine the berthing velocity of the scenarios and shown in Fig. 5. In the curve, berthing velocities are classified according to the environmental conditions of the place where the berthing structure located and the easy of navigation condition.

3.2 Selection of the scenarios

In order to determine the berthing scenario, the values of the berthing parameters elaborated in the previous section. In addition to berthing parameters, the details of the vessels, fender, and berthing structure are also needed for the scenario. In the present section, the parameters mentioned earlier and the concept of making total scenarios are introduced.

3.2.1 LNG carrier information

The dimension and mass properties of the LNG-carrier (Lee 2008) used in this study are shown in Table 1. This LNG-carrier is defined as the original vessel, and the 10 transformed vessels are generated using a geometric similarity from the original vessel with respect to the 10 selected DWT. The method of selecting DWT will be dealt with in section 3.2.4, and three vessels are generated per

Table 2 Scale controlled LNG-carrier's data

No.	DWT, M_{DWT} [t]	Volumetric displacement, V_D [m^3] Confidence limit 50%	Confidence limit 75%	Confidence limit 95%
1	14,100	22,910	25,570	30,130
2	32,300	47,470	53,120	62,530
3	58,000	79,380	88,970	104,670
4	72,000	96,030	107,700	126,680
5	101,900	130,290	146,290	172,000
6	144,000	176,690	198,600	233,410
7	216,000	252,430	284,080	333,710
8	288,000	325,130	366,210	430,060
9	360,000	395,650	445,950	523,560
10	437,200	469,370	529,340	621,340

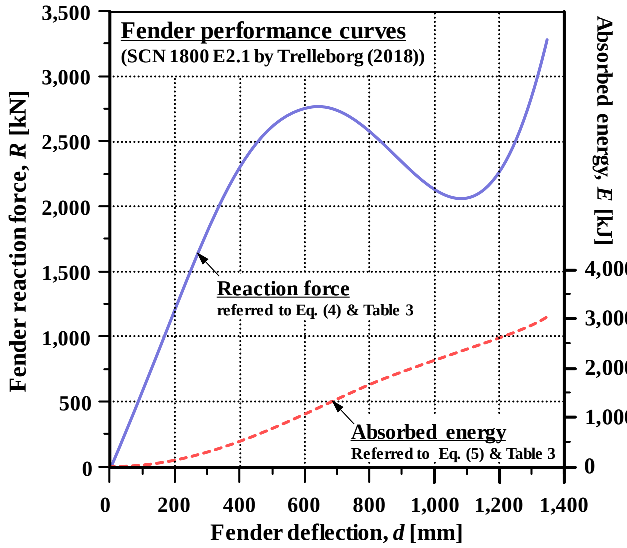

Fig. 6 Fender performance curves

each DWT using a relation between a DWT and volumetric displacement as shown in Eqs. (1)-(3). The volumetric displacements are summarized in Table 2.

3.2.2 Fender information

The fender used in this study is the Super Cone Fender (SCN) as proposed in the brochure (Trelleborg 2018). The information of the fender is usually given as a performance curve along with the basic properties. The performance curve of the fender is shown in Fig. 6. The x-axis of the curve is the deflection of the fender, the left y-axis is the reaction force of the fender in response to the deflection and the right y-axis is the berthing energy according to the deflection. The absorbed energy by the fender, E, and fender reaction force, R, are commonly expressed by fifth-order polynomial respect to the fender deflection, d. The approximated fender performances are approximated by the Eqs. (4)-(5).

For the fender reaction force, R [kN]

$$R(d) = a_1 + a_2 d + a_3 d^2 + a_4 d^3 + a_5 d^4 + a_6 d^5 \qquad (4)$$

Table 3 Coefficient of polynomial equation

Coefficient	Value	Coefficient	Value
a_1	10.9	b_1	-1.44
a_2	4.79	b_2	0.188
a_3	1.10 x 10^{-2}	b_3	1.67 x 10^{-3}
a_4	-2.73 x 10^{-5}	b_4	5.20 x 10^{-6}
a_5	1.49 x 10^{-8}	b_5	-7.66 x 10^{-9}
a_6	-1.20 x 10^{-12}	b_6	2.76 x 10^{-12}

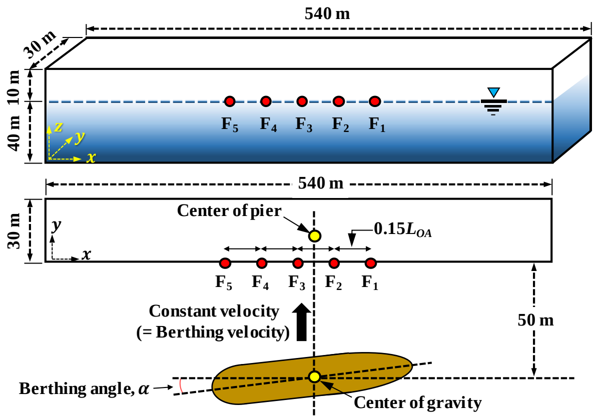

Fig. 7 Configuration of ship's berthing to the berthing structure

For the absorbed energy, E [kJ]

$$E(d) = b_1 + b_2 d + b_3 d^2 + b_4 d^3 + b_5 d^4 + b_6 d^5 \tag{5}$$

where d is the fender deflection (mm), a_1 to a_6, and b_1 to b_6 are the coefficients of the polynomial. The coefficients of equations are summarized in Table 3. These equations are inputted in ANSYS-AQWA for the fender modeling.

3.2.3 Berthing structure information

The berthing structure is modeled as a wall structure with five fenders and environmental loads are not considered. The fenders are located with an interval of 15% of the overall length of the ship's hull, L_{OA}, and this is a recommended maximum value by the guideline (BS6349-4 2014). The initial position of the vessel is 50m apart from the berthing structure and the vessel approaches the structure while keeping the initial berthing angle, α, and berthing velocity, V_B. The detailed set-up of the berthing structures is depicted in Fig. 7.

3.2.4 Total scenarios

In order to investigate the relation between the berthing energy and berthing parameters, it is desirable to simulate every combination of the parameters. However, this method is too time-consuming. Hence, the Latin Hypercube Sampling (LHS) technique (Ye 1998) is adopted. With regard to the LHS technique, several studies (Paik *et al.* 2012, Wong and Kim, 2018, Kim *et al.* 2013a, b, 2014, 2019) have been adopted this method to select reliable scenarios by adopting relevantly minimized number of scenarios with higher efficiency.

To utilize the LHS technique, the 10 DWTs and berthing angles are corresponding obtained from ten equally spaced

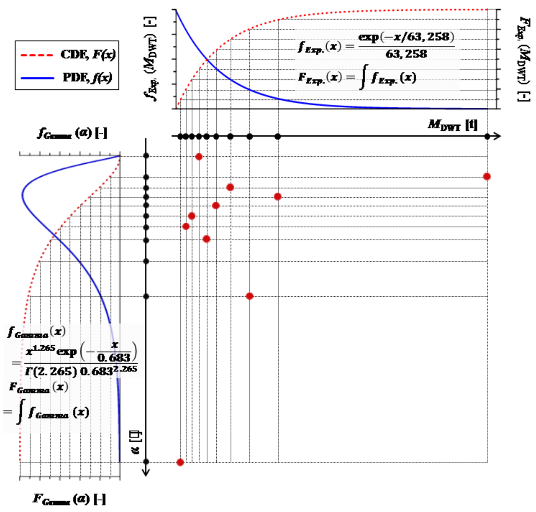

(a) Original LHS sampling

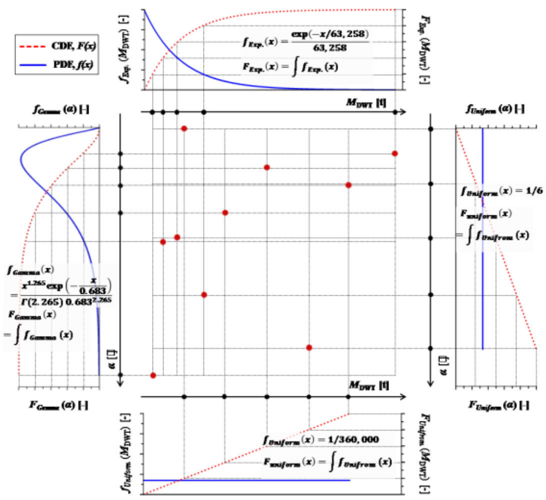

(b) Modified LHS sampling

Fig. 8 Scenarios selection using LHS technique

CDF which are integral of the PDF proposed in the previous section. This may not be the exactly same way to select scenarios, however, because of the regressed PDF's statistical characteristics, the combinations of the selected berthing angles and DWTs are gathered in the small berthing and DWT area as shown in Fig. 8(a). This implies that the scenario variety will be limited. As a solution, several berthing angles and DWTs have replaced the values derived from its Uniform PDFs. This illustrated in Fig. 8(b).

The volumetric displacement and berthing velocity are dependent on the DWT. Therefore, the number of cases is decreased from 1500 (combination of 10 DWTs, 10 berthing angles, 3 confidence limit levels, and 5 velocities) to 150 (combination of 10 DWT-berthing angles, 3 confidence limit levels, and 5 velocities). The total number of cases is summarized in Table 4.

3.3 Modelling and the calculation of the berthing energy

The steps for calculating the berthing energy are divided into two methods.

Table 4 Total scenarios details

No.	DWT, M_{DWT} [t]	Berthing Angle, α [^{0}]	Berthing velocity, V_B [m/s] Good Sheltered	Difficult Sheltered	Easy Exposed	Good Exposed	Difficult Exposed	Volumetric displacement, V_D [m^3] Confidence limit 50%	Confidence limit 75%	Confidence limit 95%
1	14,100	6.68	0.400	0.339	0.257	0.172	0.084	23,000	26,000	30,000
2	32,300	3.00	0.301	0.258	0.193	0.129	0.062	47,000	53,000	63,000
3	58,000	2.28	0.244	0.209	0.155	0.104	0.049	79,000	89,000	105,000
4	72,000	0.00	0.226	0.193	0.143	0.095	0.045	96,000	108,000	127,000
5	101,900	4.50	0.200	0.170	0.125	0.083	0.038	130,000	146,000	172,000
6	144,000	1.58	0.177	0.149	0.108	0.072	0.033	177,000	199,000	233,000
7	216,000	1.10	0.153	0.127	0.092	0.060	0.027	252,000	284,000	334,000
8	288,000	6.00	0.139	0.113	0.081	0.053	0.023	325,000	366,000	430,000
9	360,000	1.50	0.129	0.103	0.074	0.048	0.020	396,000	446,000	524,000
10	437,200	0.69	0.120	0.095	0.068	0.043	0.018	469,000	529,000	621,000

3.3.1 Conventional method

In the case of berthing energy calculation by using the kinetic energy method, each coefficient of the equation is determined according to berthing conditions. Eq. (6) shows an equation for calculating the berthing energy based on the kinetic energy method.

$$E_N = 0.5 M_D V_B^2 C_M C_E C_C C_S \tag{6}$$

where E_N is the normal berthing kinetic energy of the vessel to be absorbed by the fender (kJ), M_D is the ship's mass displacement (t), V_B is the berthing linear velocity perpendicular to the fendering line (m/s), C_M is the added mass coefficient, C_E is the eccentricity coefficient, C_C is the berthing configuration coefficient and C_S is the softness coefficient. Different guidelines may suggest different terms for the estimation of berthing energy. The detailed explanation of each parameter is described as follows.

- *Added mass coefficient*

The added mass coefficient represents the effect of the virtual mass of the ship during berthing. The method for the calculation can be represented by the three methods as shown below. The water depth and the draft of the ship are the main factors of the equation.

PIANC method (PIANC 2002)

$$C_M = \begin{cases} 1.8 & \text{for } \dfrac{K_c}{D} \le 0.1 \\ 1.875 - 0.75\left(\dfrac{K_c}{D}\right) & \text{for } 0.1 \le \dfrac{K_c}{D} \le 0.5 \\ 1.5 & \text{for } \dfrac{K_c}{D} \ge 0.5 \end{cases} \tag{7}$$

Ueda method (Ueda 1981)

$$C_M = 1 + \frac{\pi D}{2 C_B B} \quad \text{where} \quad C_B = \frac{M_D}{L_{BP} B D \rho_{SW}} \tag{8}$$

Vasco Costa method (Vasco Costa 1964)

$$C_M = 1 + \frac{2D}{B} \tag{9}$$

Where K_C is the under-keel clearance (m), C_B is the block coefficient, D is the draft of a vessel (m), B is the breadth of a vessel (m), L_{BP} is the length between perpendiculars (m), and ρ_{SW} is the seawater density (1,025 kg/m^3). PIANC method (PIANC 2002) is only valid when V_B is larger than 0.08 m/s and K_C is larger than 0.1 times the draft.

- *Eccentricity coefficient*

The eccentricity coefficient is used for describing the amount of dissipated energy by the rotation of the ship during berthing on the fender. Usually, C_E varies between 0.3 to 1.0 for different berthing angles and conditions, which can be estimated throughout Eqs. (10)-(12) according to the contact-point location on the ship.

Quarter-point berthing

$$C_E = 0.4 \sim 0.6 \quad \text{when} \quad x = L_{BP}/4 \tag{10}$$

Third-point berthing

$$C_E = 0.6 \sim 0.8 \quad \text{when} \quad x = L_{BP}/3 \tag{11}$$

Midships berthing

$$C_E = 1.0 \quad \text{when} \quad x = L_{BP}/2 \tag{12}$$

where x is the distance from the bow to the contact point. In this research, the maximum value of C_E is used in each simulation to obtain conservative berthing energy.

- *Softness coefficient*

This coefficient is determined by the ratio between the elasticity of the fender system and that of the hull. If the fender is too hard, the hull will experience deformation. In general, the C_S is 1.0 and 0.9 for a soft fender and a harder fender respectively. The C_S is set at 1.0 in the simulations as the hull is assumed to be a rigid body in ANSYS-AQWA.

- *Berthing configuration coefficient*

The cushion effect caused by the trapped water between the berthing structure and the hull differs with the configuration of the berthing structure, which can be referred to as the berthing configuration coefficient (C_C). This coefficient is determined based on berthing angle, berthing, the configuration of the berthing structure, and the under-keel clearance. A typical method determining C_C is elaborated as follows:

Table 5 Berthing coefficients corresponding to the numerical simulations

No.	CM	C_M Method	C_M	C_C	C_S	C_E Confidence limit 50%	C_E Confidence limit 75%	C_E Confidence limit 95%
1	1	PIANC Method	1.500	1.0	1.0	0.6	0.6	0.6
2			1.500	1.0	1.0	0.6	0.8	0.8
3			1.500	1.0	1.0	0.8	0.8	0.8
4			1.500	1.0	1.0	1.0	1.0	1.0
5			1.500	1.0	1.0	0.6	0.6	0.6
6			1.500	1.0	1.0	0.8	0.8	0.8
7			1.500	1.0	1.0	1.0	1.0	0.8
8			1.500	1.0	1.0	0.6	0.6	0.6
9			1.500	1.0	1.0	1.0	0.8	0.8
10			1.500	1.0	1.0	1.0	1.0	1.0
1	2	Ueda Method	1.582	1.0	1.0	0.6	0.6	0.6
2			1.581	0.9	1.0	0.6	0.8	0.8
3			1.581	0.9	1.0	0.8	0.8	0.8
4			1.581	0.9	1.0	1.0	1.0	1.0
5			1.581	0.9	1.0	0.6	0.6	0.6
6			1.581	0.9	1.0	0.8	0.8	0.8
7			1.581	0.9	1.0	1.0	1.0	0.8
8			1.581	1.0	1.0	0.6	0.6	0.6
9			1.581	0.9	1.0	1.0	0.8	0.8
10			1.581	0.9	1.0	1.0	1.0	1.0
1	3	Vasco Costa Method	1.549	1.0	1.0	0.6	0.6	0.6
2			1.549	0.9	1.0	0.6	0.8	0.8
3			1.549	0.9	1.0	0.8	0.8	0.8
4			1.549	0.9	1.0	1.0	1.0	1.0
5			1.549	0.9	1.0	0.6	0.6	0.6
6			1.549	0.9	1.0	0.8	0.8	0.8
7			1.549	0.9	1.0	1.0	1.0	0.8
8			1.549	1.0	1.0	0.6	0.6	0.6
9			1.549	0.9	1.0	1.0	0.8	0.8
10			1.549	0.9	1.0	1.0	1.0	1.0

- For open berths, corner of quay walls with berthing angle is larger than 5°, C_C is taken as 1.0

- For solid quay walls under a parallel approach with under-keel clearance less than 15% of the vessel draught, C_C is taken as 0.9

The berthing coefficients obtained for each case are summarized in Table 5, and the results from berthing energy calculation by using the conventional method are shown in Table 6. According to Tables 5 and 6, CM refers to the combination of conventional methods.

3.3.2 Numerical method

In the ANSYS-AQWA, the berthing structures and vessel are modeled as described in section 3.2.3, and a time-domain berthing analysis is simulated. However, the fluid non-linearity like the water cushion effect can't be simulated because of its theory limitation.

During the berthing simulation, the first contact between the ship and the fender occurs at Fender1 unless the berthing angle is zero. After the first collision, the consecutive collisions on other fenders occur due to the ship's rotation by the fender's reaction forces or the inertia forces by the berthing acceleration. The number of fenders colliding with the ship and time delay of 2nd collision is depending on the initial conditions such as the DWT, the berthing angle, and the berthing velocity. Briefly, the collisions can be divided into two groups as illustrated in Figs. 9(a) and (b).

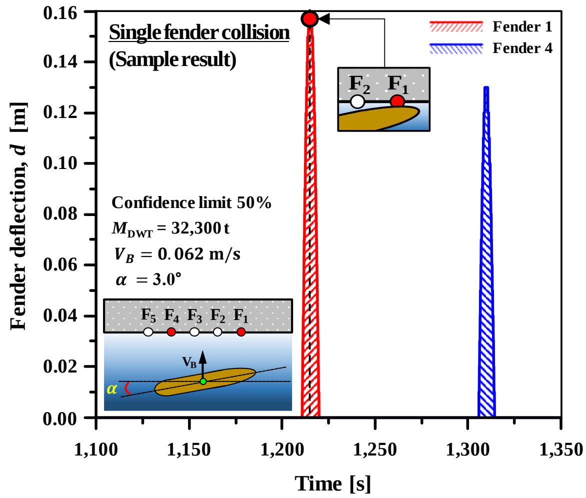

(a) Single fender collision

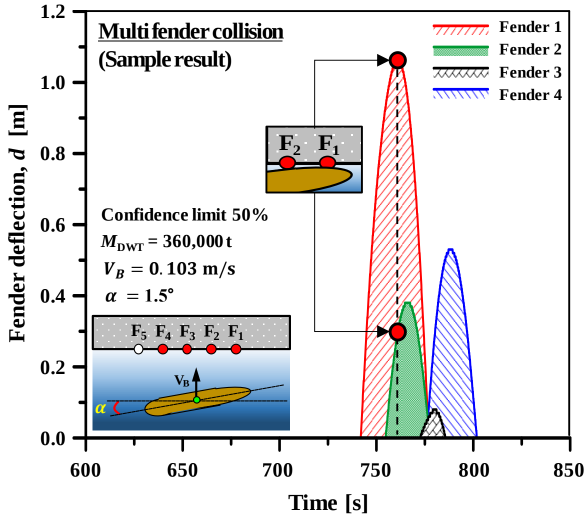

(b) Multi fender collision

Fig. 9 Example of numerical simulation result

In the case of the single fender collision in Fig. 9(a), there are no other fender collisions when the maximum deflection is observed at the Fender1. After the maximum deflection at the Fender 1, the kinetic energy loss of the ship occurs due to the structural damping of the fender and the hydrodynamic damping around the vessel. Therefore, the berthing energy is calculated with the maximum deflection of Fender1 using Eq. (5), and this is defined as the berthing energy by calculated the numerical method.

On the other hand, in the multi fender collision as in Fig. 9(b), several fenders are colliding with the vessel when the Fender1 deflected most in the multi fender collision.

Table 6 Berthing energy calculation result by the conventional method

DWT [t]	Berthing velocity, V_B [m/s]	Berthing energy, E_N (x 10^3) [kJ]								
		Confidence limit 50%			Confidence limit 75%			Confidence limit 95%		
		CM1	CM2	CM3	CM1	CM2	CM3	CM1	CM2	CM3
	0.400	1.706	1.799	1.762	1.904	2.008	1.966	2.246	2.368	2.320
	0.339	1.225	1.292	1.265	1.368	1.442	1.412	1.613	1.701	1.666
14,100	0.257	0.704	0.743	0.727	0.786	0.829	0.812	0.927	0.978	0.958
	0.172	0.315	0.333	0.326	0.352	0.371	0.364	0.415	0.438	0.429
	0.084	0.075	0.079	0.078	0.084	0.089	0.087	0.099	0.104	0.102
	0.301	2.005	1.902	1.863	2.992	2.838	2.781	3.522	3.340	3.273
	0.258	1.473	1.397	1.369	2.198	2.085	2.043	2.587	2.454	2.405
32,300	0.193	0.824	0.782	0.766	1.230	1.167	1.143	1.448	1.373	1.346
	0.129	0.368	0.349	0.342	0.550	0.521	0.511	0.647	0.614	0.601
	0.062	0.085	0.081	0.079	0.127	0.120	0.118	0.149	0.142	0.139
	0.244	2.937	2.786	2.730	3.292	3.123	3.060	3.874	3.674	3.600
	0.209	2.155	2.044	2.003	2.415	2.291	2.245	2.842	2.696	2.642
58,000	0.155	1.185	1.124	1.102	1.329	1.260	1.235	1.563	1.483	1.453
	0.104	0.534	0.506	0.496	0.598	0.567	0.556	0.704	0.667	0.654
	0.049	0.118	0.112	0.110	0.133	0.126	0.123	0.156	0.148	0.145
	0.226	3.811	3.614	3.542	4.273	4.053	3.972	5.028	4.769	4.673
	0.193	2.779	2.636	2.583	3.116	2.956	2.897	3.667	3.478	3.408
72,000	0.143	1.526	1.447	1.418	1.711	1.623	1.590	2.013	1.909	1.871
	0.095	0.673	0.639	0.626	0.755	0.716	0.702	0.888	0.843	0.826
	0.045	0.151	0.143	0.140	0.169	0.161	0.157	0.199	0.189	0.185
	0.200	2.430	2.305	2.258	2.728	2.588	2.536	3.208	3.043	2.982
	0.170	1.756	1.665	1.632	1.971	1.870	1.832	2.318	2.198	2.154
101,900	0.125	0.949	0.900	0.882	1.066	1.011	0.991	1.253	1.189	1.165
	0.083	0.418	0.397	0.389	0.470	0.446	0.437	0.553	0.524	0.514
	0.038	0.088	0.083	0.082	0.098	0.093	0.092	0.116	0.110	0.108
	0.177	3.441	3.264	3.199	3.868	3.668	3.595	4.546	4.311	4.225
	0.149	2.439	2.313	2.267	2.741	2.600	2.548	3.221	3.055	2.994
144,000	0.108	1.281	1.215	1.191	1.440	1.366	1.338	1.692	1.605	1.573
	0.072	0.569	0.540	0.529	0.640	0.607	0.595	0.752	0.713	0.699
	0.033	0.120	0.113	0.111	0.134	0.128	0.125	0.158	0.150	0.147
	0.153	4.592	4.355	4.268	6.071	5.758	5.643	4.857	4.606	4.514
	0.127	3.164	3.000	2.940	4.183	3.967	3.888	3.346	3.174	3.110
216,000	0.092	1.660	1.575	1.543	2.195	2.082	2.040	1.756	1.666	1.632
	0.060	0.706	0.670	0.656	0.934	0.886	0.868	0.747	0.708	0.694
	0.027	0.143	0.136	0.133	0.189	0.179	0.176	0.151	0.143	0.141
	0.139	2.929	3.087	3.025	3.299	3.476	3.407	3.875	4.083	4.001
	0.113	1.936	2.040	1.999	2.180	2.298	2.252	2.561	2.698	2.644
288,000	0.081	0.995	1.048	1.027	1.120	1.181	1.157	1.316	1.386	1.359
	0.053	0.426	0.449	0.440	0.480	0.505	0.495	0.563	0.594	0.582
	0.023	0.080	0.085	0.083	0.090	0.095	0.093	0.106	0.112	0.110
	0.129	5.117	4.853	4.756	4.614	4.376	4.288	5.417	5.137	5.035
	0.103	3.262	3.094	3.032	2.941	2.790	2.734	3.453	3.275	3.210
360,000	0.074	1.684	1.597	1.565	1.518	1.440	1.411	1.783	1.690	1.657
	0.048	0.708	0.672	0.658	0.639	0.606	0.594	0.750	0.711	0.697
	0.020	0.123	0.117	0.114	0.111	0.105	0.103	0.130	0.123	0.121
	0.120	5.253	4.982	4.882	5.924	5.618	5.506	6.953	6.594	6.463
	0.095	3.292	3.122	3.060	3.713	3.521	3.451	4.358	4.133	4.050
437,200	0.068	1.687	1.600	1.568	1.902	1.804	1.768	2.233	2.118	2.075
	0.043	0.674	0.640	0.627	0.761	0.721	0.707	0.893	0.847	0.830
	0.018	0.118	0.112	0.110	0.133	0.126	0.124	0.156	0.148	0.145

The ship's kinetic energy is absorbed by all colliding fenders; the berthing energy is calculated by summing all the absorbing energy of colliding fenders when the maximum deflection occurs at Fender1. The analysis results are summarized in Table 7.

3.4 Statistical analysis

The calculated berthing energies from the above two methods are compared by statistical analysis. In addition,

Table 7 Berthing energy computational result by ANSYS-AQWA

DWT [t]	Berthing Velocity, V_B [m/s]	Berthing energy, E_N (x 10^3) [kJ] Confidence limit		
		50%	75%	95%
14,100	0.400	1.635	1.824	2.360
	0.339	1.143	1.260	1.613
	0.257	0.633	0.705	0.871
	0.172	0.285	0.318	0.388
	0.084	0.076	0.085	0.102
32,300	0.301	2.087	2.347	2.807
	0.258	1.480	1.677	2.056
	0.193	0.794	0.894	1.098
	0.129	0.356	0.396	0.480
	0.062	0.091	0.101	0.120
58,000	0.244	2.392	2.784	3.170
	0.209	1.716	2.042	2.369
	0.155	0.903	1.068	1.245
	0.104	0.403	0.476	0.548
	0.049	0.100	0.116	0.131
72,000	0.226	3.769	4.348	5.370
	0.193	2.707	3.123	3.799
	0.143	1.489	1.707	2.041
	0.095	0.690	0.786	0.928
	0.045	0.186	0.209	0.244
101,900	0.200	2.807	3.053	3.630
	0.170	2.020	2.229	2.691
	0.125	1.026	1.152	1.400
	0.083	0.445	0.495	0.591
	0.038	0.105	0.116	0.137
144,000	0.177	2.936	3.684	4.140
	0.149	2.122	2.424	2.978
	0.108	1.083	1.251	1.456
	0.072	0.473	0.534	0.615
	0.033	0.108	0.125	0.137
216,000	0.153	3.727	5.277	4.661
	0.127	2.425	2.868	3.521
	0.092	1.137	1.278	1.584
	0.060	0.476	0.534	0.649
	0.027	0.105	0.115	0.138
288,000	0.139	3.411	3.813	4.638
	0.113	2.304	2.602	3.182
	0.081	1.131	1.293	1.638
	0.053	0.469	0.526	0.657
	0.023	0.098	0.109	0.133
360,000	0.129	4.226	4.659	5.021
	0.103	2.584	3.013	3.324
	0.074	1.164	1.347	1.716
	0.048	0.473	0.553	0.675
	0.020	0.096	0.111	0.131
437,200	0.120	5.661	6.434	6.392
	0.095	2.981	3.593	3.978
	0.068	1.282	1.509	1.767
	0.043	0.471	0.569	0.681
	0.018	0.093	0.106	0.127

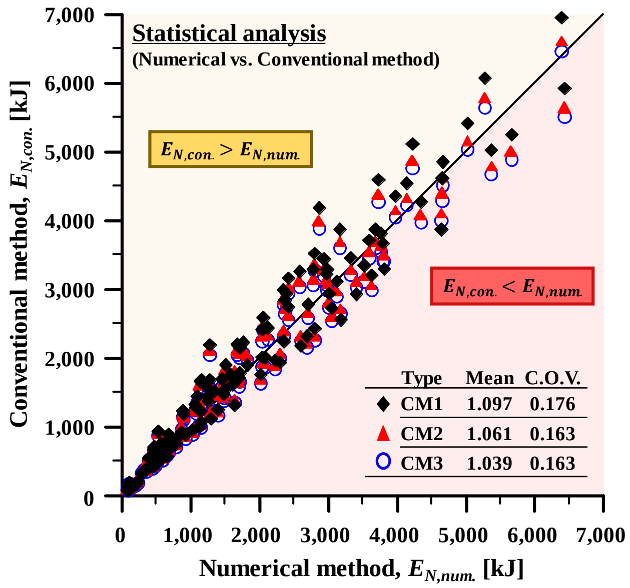

Fig. 10 Comparison of conventional and numerical methods

the sensitivity of berthing energy according to each parameter is also investigated.

3.4.1 Comparison results between the two methods

The result obtained from the combination of three conventional methods is compared to that of the numerical simulation. A statistical method is used to determine the degree of matching between the methods. The mean, which is an average obtained by dividing the conventional method results by the numerical results, represents the difference between two methods. The covariance, which is another statistical value, represents the degree of deviation between the two methods. Therefore, if the mean is near to 1 and the covariance is smaller, the compatibility of both methods is high. The results are shown in Fig. 10. The lower area of the graph is representing the results when the berthing energy of the numerical method is larger than that of the conventional methods. On the other hand, the upper area of the graph is for the opposite cases.

Depending on the combination, the mean varies approximately from 4% to 10%. This means that the conventional method generally overestimated the berthing energy than that of the numerical method. However, in some cases, the berthing energy by the numerical method is larger than the result of the conventional method. In addition, conventional methods show different results to each other. The CM1 shows the highest mean and covariance, which implies that the CM1 is most conservative among the methods. On the other hand, CM3 shows the least mean and covariance. The difference between these methods is because of the definition of C_M. PIANC method (PIANC 2002) in CM1 is the equation considering the water cushion effect.

However, CM3 which is VASCO COSTA method (VASCO COSTA 1964) only considered the geometry of a vessel for C_M. In this study, the non-linear term was not considered in the numerical method, therefore CM3 shows better agreement with numerical method than CM1.

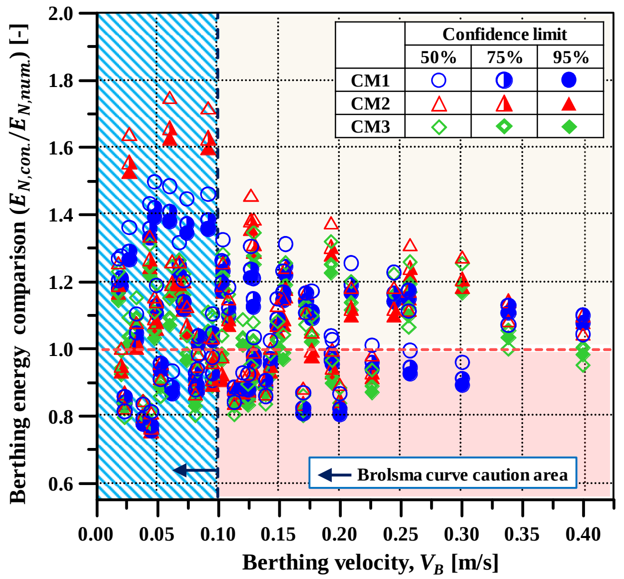

(a) Berthing energy comparison verse to berthing velocity

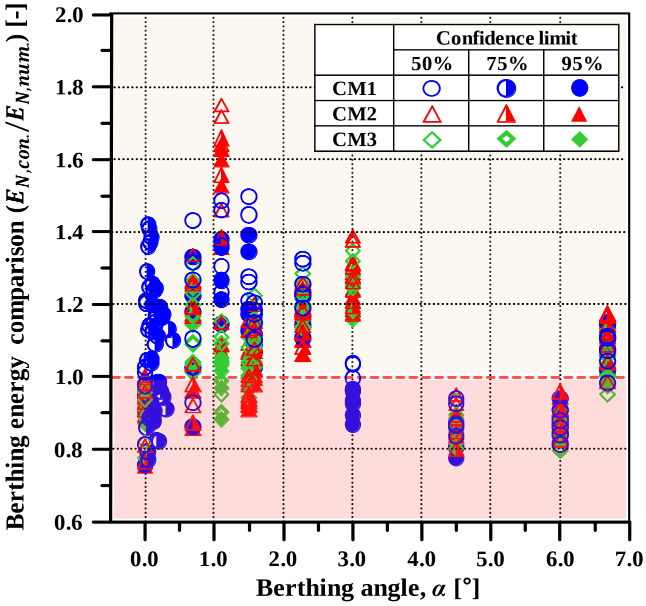

(b) Berthing energy comparison verse to berthing angle

Fig. 11 Comparison result between two methods according to the berthing parameters.

3.4.2 Parameter sensitivity result

From the comparison results between conventional methods and numerical method, the covariance of each method shows somewhat a larger value. To reveal the reason for it, the tendency of differences between the two methods is investigated according to each parameter. The berthing energy comparison with respect to berthing velocity at different confident limit levels is illustrated in Fig. 11(a).

When the comparison is analyzed from the viewpoint of the berthing velocity, there is a difference between the two methods throughout all berthing velocity. However, the difference at the relatively low berthing velocity is larger than the relatively high berthing velocity. Especially, a significant difference is observed especially in the velocity range that is not recommended for the Broslma curve (extremely low berthing velocity). Since the uncertainty of the currently used method increases in the low-speed section, a higher safety factor value is required to be applied on the existing method to the low-speed berthing velocity than the other berthing velocity berthing. On the other hand, there is no significant tendency of differences in respect to the confidence limit.

In the case of the berthing angle, the tendency of differences between the two methods is shown in Fig. 11(b) according to the berthing angle and confidence limit levels. The difference between the two methods is large at a relatively low berthing angle. The greater the angle, the higher the compatibility of the two methods. Usually, the conventional method is designed to estimate berthing energy larger than the real values. In this aspect, in the large berthing angle area, the conventional method is less conservative. On the other hand, the tendency of difference according to the volumetric displacement is rather random. In other words, the size of the vessel itself has little effect on the difference between the two methods. As a summary, the conventional methods show similarity with the numerical method in a region of the relatively large berthing angle and velocity.

3.5 Propose the refined safety factor

3.5.1 Abnormal and normal berthing energy

When designing the berthing structures, the conventional method is defined as normal berthing energy. However, in an actual berthing procedure, there are many factors affecting berthing; human error, malfunction, exceptional weather etc. In the aspect of the berthing structure design, the safety factors are used to cover these problems. The berthing energy considered these uncertainties is referred to as abnormal berthing energy which can be calculated by Eq. (13).

$$E_A = F_S E_N \tag{13}$$

As used herein, E_N is the normal berthing energy to be absorbed by the fender (kJ), F_S is the safety factor and E_A is the abnormal berthing energy (kJ). The safety factor varies depending on the vessel type and size. The safety factors used in design codes are shown in Table 8. The safety factor for the LNG-carrier is recommended to be 2.0 in ROM, EAU, and BS 6349 (ROM 1990, Grabe 2012, BS6349-4 2014) while PIANC (PIANC 2002) suggests either 1.25 or 1.75 depending on vessel size. However, there are no clear criteria for the size.

Table 8 Factors of safety for main vessel.

Type of vessel	Size	Safety factor, F_S [-] PIANC	ROM	EAU	BS 6349
Tanker, bulk and cargo	Largest	1.25	2.0	2.0	Up to 2.0
	Smallest	1.75			
Container	Largest	1.5	2.0	2.0	Up to 2.0
	Smallest				

Table 9 Optimized safety factor by Versteegt (2013)

Type of vessel	Size	Safety factor, F_S [-]
Tanker, bulk and cargo	Largest	1.30
	Smallest	1.75
LNG carriers	up to 80,000 t	1.2
Container	Largest	1.5
	Smallest	2.0

3.5.2 Refined safety factor

In section 3.4, the conservativeness of conventional methods is shown. The conservativeness of the abnormal berthing energy will be higher than that of normal berthing energy. To mitigate this conservativeness, a proper range of the safety factor is proposed from that existing conservative safety factor. The initial range of a refined safety factor is referring to guidelines. The new safety factor has an upper limit set to be 1.75 and a lower limit set to be 1.25. Based on the comparison results in the previous section, the CM3, which is the least conservative and most compatible with the numerical method, is set as the representative conventional method and normal berthing energy. The results of the abnormal berthing energy using the guidelines and refined safety factors are shown in Figs. 12(a) and (b).

As illustrated, the safety factor is divided depending on the DWT, and the results obtained from the comparison are divided into two groups. In Fig. 12(a), the results obtained from comparison for a relatively small vessel are plotted. On the other hand, in Fig. 12(b), the results for a relatively large vessel are plotted. Regardless of the DWT, both cases show similar results, in which there is no significant relationship observed between the safety factor and the ship size. As seen from the graph, when the safety factor, F_S is 1.75 and 2.0, results are too conservative, and some abnormal berthing energy is over 3 times than the corresponding numerical method result. As some cases show a large deviation, hence it is not easy to decide a specific F_S. However, in the range of 1.4 to 1.6, all results obtained from the comparison exceed the value 1, which implies that the results are converged. For a safe design of berthing structure, a safety factor, F_S of 1.5 or 1.6 is sufficient. This result is rather higher than that of previous optimized results in Table 9 but is narrower and smaller than the existing safety factors in Table 8.

4. Concluding remarks

The present research is motivated by the conventional berthing energy calculation method, which based on lots of assumptions and is outdated. As an alternative way, the numerical method is used for calculating the berthing energy, and it compared with the conventional methods. In addition, based on the comparison results, a new range of the safety factor is suggested. The important results are as follows.

- The existing methods are classified into three methods according to the berthing coefficient calculation method in this study. According to the comparison, although

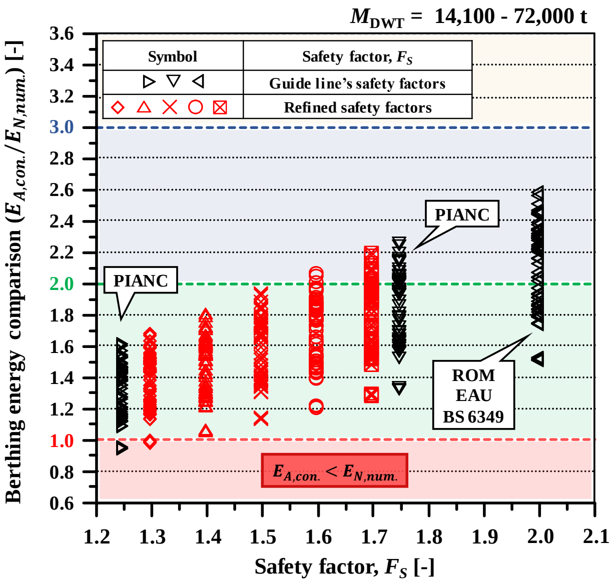

(a) Deadweight tonnage, M_{DWT} = 14,100 to 72,000 t

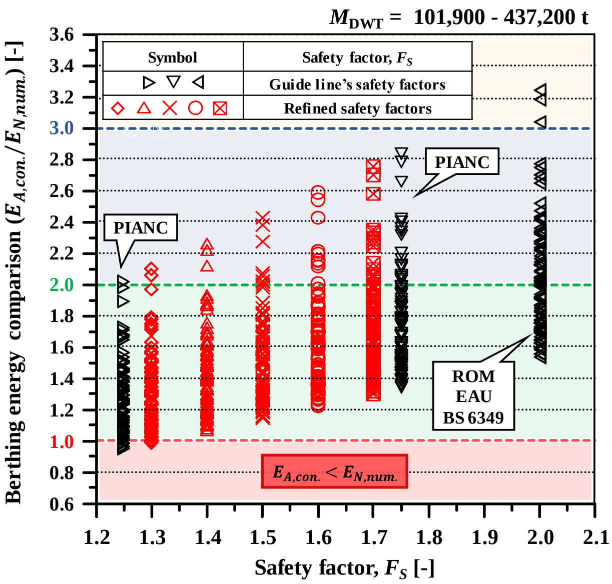

(b) Deadweight tonnage, M_{DWT} = 101,900 to 437,200 t

Fig. 12 Abnormal berthing energy comparison with numerical method

there are some variations, the berthing energies by calculated the conventional methods are 4% to 10% larger than the result of the simulation.

- From the results of the berthing parameter sensitivity test, the error between the two methods occurs largely in the low berthing velocity area. Also, the conservativeness of the conventional method is low in the high berthing angle section. Considering that the berthing velocity lowers as the vessel size increases, certain care must be taken to estimate the berthing energy of the low berthing velocity area.
- The safety factors proposed in the guideline are varied according to vessel size, but the criteria for subdividing the ship's size are ambiguous. From the safety factor refining results, the range of the new safety factor is between 1.4 and 1.6 regardless of DWT.

The conventional methods are simpler and faster than numerical simulation. However, from the viewpoint of design optimization, it is necessary to design the berthing structure reasonably to avoid excessive design and reduce the design cost. Therefore, it is necessary to enhance the existing methods and safety factor to prevent excessive design. The result of this study can be extended through applications to various vessels with realistic modeling of the berthing structures. Also, a consideration of environmental loads can implement the non-linear effect of berthing energy estimation.

Acknowledgements

The authors would like to thank Daewoo E&C, Republic of Korea for their kind support. This research was supported by the Technology Innovation Program (Grant No.: 10053121) funded by the Ministry of Trade, Industry & Energy (MI, Korea).

References

ANSYS (2013), Aqwa Theory Manual; Release 15.0; ANSYS Inc., Canonsburg, PA, USA. http://www.ansys.com

Brolsma, J.V., Hirs, J.A. and Langeveld, J.M. (1977), "On the fender design and berthing velocities", *PIANC 24th International Navigation Congress*, Leningrad, Russia, March.

BS6349-4 (2014), Maritime works - Part4. Code of practice for 52 design of fendering and mooring systems, British Standards 53 Institution; London, United Kingdom.

Burkhart, E.C. and Matakis, K.E. (2013), "Collection of berthing velocities and resulting design recommendations by PIANC Working Group MarCom 145", *ASCE PORTS 2013*, Seattle, Washington, USA, August.

Chen, M. and Chen, H.C. (1996), "Numerical simulation of transitional flows induced by a berthing ship", *J. Offshore Polar Eng.*, **7**(4), 277-284.

Clarkson (2014), Clarksons Research; http://www.crsl.com

Fontijn H.L. (1988), "Fender forces in ship berthing", Research Report No. 88-2; Department of Civil Engineering, Delft University of Technology, Delft, Netherlands.

Girgrah, M. (1977), "Practical aspects of dock fender design", *PIANC 24th International Navigation Congress*, Leningrad, Russia, March.

Grabe J. (2012), *Recommendations of the Committee for Waterfront Structures Harbours and Waterways EAU 2012*, (9th Edition), John Wiley and Sons, Hamburg, Germany.

Headland, J.R. (1992a), "Design of Fender systems using a numerical berthing model", Permanent International Association of Navigation Congresses Bulletin No.77.

Headland, J.R. (1992b), "A Computational berthing model for the design of fender systems", *ASCE Proceedings Specialty conference PORTS'92*, Seattle, Washington, USA, July.

Hein, C. (2014) "Berthing velocity of large container ships", *PIANC 33th International Navigation Congress*, San Francisco, USA, June.

Kim, D.K., Kim, B.J., Seo, J.K., Kim, H.B., Zhang, X.M. and Paik, J.K. (2014), "Time-dependent residual ultimate longitudinal strength-grounding damage index (R-D) diagram", *Ocean Eng.*, **76**, 163-171.

Kim, D.K., Kim, H.B., Park, D.H., Mohd, M.H. and Paik, J.K. (2019), "A practical diagram to determine the residual longitudinal strength of grounded ship in Northern Sea Route", *Ships Offshore Struct.*, **15**(7), https://doi.org/10.1080/17445302.2019.1667113.

Kim, D.K., Perdersen, P.T., Paik, J.K., Kim, H.B., Zhang, X.M. and Kim, M.S. (2013a), "Safety guidelines of ultimate hull girder strength for grounded container ships", *Safety Science*, **59**, 46-54. https://doi.org/10.1016/j.ssci.2013.04.006.

Kim, D.K., Yu, S.Y. and Choi, H.S. (2013b), "Condition assessment of raking damaged bulk carriers under vertical bending moments", *Struct. Eng. Mech.*, **46**(5), 629-644. https://doi.org/10.12989/sem.2013.46.5.629.

Kong, G.Y., Le, Y.S. and Lee, S.M. (2004), "A study on the modeling of transitional lateral force acting on the berthing ship by CFD", *Korea Soc. Mech. Eng.*, **18**(7), 1196-1202. https://doi.org/10.1007/BF02983294.

Lee, S.J. (2008), "The effects of LNG-sloshing on the global responses of LNG-carriers", Ph.D. Dissertation, Texas A&M University, Texas.

Magda, W. (2019), "Elastic fender-dolphin interaction for economic design of berthing dolphins", *J. Waterway, Port, Coastal, Ocean Eng.,* **145**(3), 0419007. https://doi.org/10.1061/(ASCE)WW.1943-5460.0000511.

Metzger, A.T., Hutchinson, J. and Kwiatkowski, J. (2014), "Measurement of marine vessel berthing parameters", *Marine Struct.*, **39**, 350-372. https://doi.org/10.1016/j.marstruc.2014.10.001.

Mostofi, A. and Bargi, K. (2012), "New concept in analysis of floating piers for ship berthing impact", *Marin Struct.*, **25**(1), 58-70. https://doi.org/10.1016/j.marstruc.2011.12.001.

Neser, G. and Unslan, D. (2006), "Dynamics of ships and fenders during berthing in a time domain", *Ocean Eng.*, **33**(14-15), 1919-1934. https://doi.org/10.1016/j.oceaneng.2005.10.020.

Paik, J.K., Kim, D.K., Park, D.H., Kim, H.B. and Kim, M.S. (2012), "A new method for assessing the safety of ships damaged by grounding", *J. Maritime Eng.*, **154**(A1), 1-20.

PIANC (2002), *Guidelines for the Design of Fender Systems: 2002,* International Navigation Association, Brussels, Belgium.

ROM (1990), "Maritime works recommendations - ROM 0.2-90 - Actions in the design of maritime and harbour works", Puertos del Estado, Madrid, Spain.

Roubos, A., Groenewegen, L. and Peters, D.J. (2017), "Berthing velocity of large seagoing vessels in the port of Rotterdam", *Marine Struct.*, **51**, 202-219. https://doi.org/10.1016/j.marstruc.2016.10.011.

Roubos, A., Peters, D.J., Groenewegen, L. and Steenbergen, R. (2018), "Partial safety factors for berthing velocity and loads on marine structures", *Marine Struct.*, **58**, 73-91. https://doi.org/10.1016/j.marstruc.2017.11.003.

Saurin, B.F. (1963), "Berthing forces of large tankers", *Proceedings of the 6th World Petroleum Congress*, Frankfurt am Main, Germany, June.

Toda, Y., Lee, Y.S. and Sadakane, H. (2002), "Numerical investigations of hydrodynamic forces acting on a ship hull under lateral low speed motion", *J. Kansai Soc. Naval Architects*, **238**, 77-83. https://doi.org/10.14856/jksna.2002.238_77.

Toppler, J.F and Weersma, J. (1973), "Planning and design of fixed-berth structures for 300,000 to 500,00 DWT tankers", *J. Petroleum Technol.*, **25**(7), 764-774. https://doi.org/10.2118/3950-PA.

Trelleborg (2018), Brochures and Catalogs; Trelleborg Coated Systems, Lodi Vecchio, Italy. https://www.trelleborg.com

Ueda S. (1981), "Study in berthing impact force of very large crude oil carriers", *Japanese Port Harbour Res. Institute*, **20**(2), 169-209.

Ueda, S., Hirano, T., Shiraishi, S., Yamamoto, S. and Yamase, S. (2002), "Reliability design of fender systems for berthing ship", *30th PIANC-AIPCN Congress 2002 on Institution of Engineers*, Sydney, Australia, September.

Vasco Costa, F. (1964), "The berthing ship. The effect of impact on the design of fenders and other structures", *The Dock Harbour Authority*, **19**(523), 524-524.

Versteegt, G. (2013), "Berthing loads in structural design", M.Sc. Dissertation, Delft University of Technology, Delft.

Wang, H., Li, X., Chen, L. and Sun, X. (2016), "Numerical study on the hydrodynamic forces on a ship berthing to quay by taking free-surface effect into account", *J. Marine Sci. Technol.*, **21**(4), 601-610. https://doi.org/10.1007/s00773-016-0376-z.

Wang, H., Sheng, X., Wang, S., Chen, L., Yuan, Z. and Wu, Q. (2017), "Numerical study on water depth effects on hydrodynamic forces acting on berthing ships", *J. Shanghai Jiaotong University (Science)*, **22**(2), 198-205. https://doi.org/10.1007/s12204-017-1822-8.

Wong, E.W.C. and Kim, D.K. (2018), "A simplified method to predict fatigue damage of TTR subjected to short-term VIV using artificial neural network", *Adv. Eng. Software*, **126**, 100-109. https://doi.org/10.1016/j.advengsoft.2018.09.011.

Yamase, S., Ueada S., Okada T., Arai A. and Shimizu K. (2014) "Characteristics of measured berthing velocity and the application for fender design of berthing ship", *PIANC 33th International Navigation Congress*, San Francisco, USA, June.

Ye, K.Q. (1998), "Orthogonal column Latin hypercubes and their application in computer experiments", *J. American Statistical Assoc.*, **93**(444), 1430-1439.

CC